Fault Detection and Severity Analysis of Servo Valves Using Recurrence Quantification Analysis

M. Samadani[1], C. A. Kitio Kwuimy[2], and C. Nataraj[3]

[1,2,3] *Department of Mechanical Engineering, Villanova University, Villanova, PA, 19085, USA*
msamadan@villanova.edu
cedrick.kwuimy@villanova.edu
nataraj@villanova.edu

ABSTRACT

This paper presents the application of recurrence plots (RPs) and recurrence quantification analysis (RQA) in model-based diagnostics of nonlinear systems. A detailed nonlinear mathematical model of a servo electro-hydraulic system has been used to demonstrate the procedure. Two faults have been considered associated with the servo valve including the increased friction between spool and sleeve and the degradation of the permanent magnet of the valve armature. The faults have been simulated in the system by the variation of the corresponding parameters in the model and the effect of these faults on the RPs and RQA parameters has been investigated. A regression-based artificial neural network has been finally developed and trained using the RQA parameters to estimate the original values of the faulty parameters and identify the severity of the faults in the system.

1. INTRODUCTION

Servo valves are complex electro-hydraulic systems which consist of very precise and sensitive components. A small change in the dimensions, metallurgical characteristics, or other parameters of these components can produce instability, error or even failure in the performance of the system. Hence, it is important to utilize effective algorithms and techniques to constantly monitor the performance of such systems and identify faults that can appear in them along with location and severity of the faults. Due to highly nonlinear characteristics of servo valves, it is essential to use techniques that can perform effectively in different domains of the nonlinear response.

In this paper, we introduce the application of recurrence plots (RPs) and recurrence quantification analysis (RQA) in model-based diagnostics of servo valves. The approach is general though and can be applied to any complex nonlinear system. Model-based fault detection approaches can be classified into three main categories of parity relation (Chow & Willsky, 1984; Gertler, 1997; Gertler & Singer, 1990), observer/filter-based (Frank & Ding, 1997; Patton, Frank, & Clarke, 1989) and parameter estimation (Isermann, 1982, 1984) methods. In parameter estimation method which is the main scope of this research, the parameters of the defective system are estimated and compared with the original parameters of the healthy system. The changes in parameter values are in many cases directly related to the defects. Therefore, this knowledge facilitates the fault diagnostics task. The parameter estimation technique has been used by many researchers for the detection of the faults in complex systems such as jet engines, rolling element bearings, DC motors, etc. (Baskiotis, Raymond, & Rault, 1979; Kappaganthu & Nataraj, 2011a; Liu, Zhang, Liu, & Yang, 2000). More information about parameter estimation based fault detection can be found in (Frank, Ding, & Koppen-Seliger, 2000; Isermann, 1997, 2005a, 2005b).

In general, nonlinear dynamic systems can exhibit diverse phenomena including multi-periodic, quasi-periodic and chaotic responses, as well as bifurcation and limit cycles. Many studies have reported the emergence of these complex nonlinear phenomena in industrial machinery originating from defects or due to their nonlinear nature (Sankaravelu, Noah, & Burger, 1994; Mevel & Guyader, 1993; Kappaganthu & Nataraj, 2011b). The prevailing parameter estimation methods are based on system identification techniques which are mostly suitable for linear systems and are not effective when the system response includes complex nonlinear phenomena. Moreover, the available methods require a pre-specified range for the initial guess of the parameter values which might not always be available in practice.

This paper presents the initial investigation of a new approach for parameter estimation-based diagnostics of nonlinear systems, based on the extracted information from the nonlinear response. Our main thesis is that the nonlinear dynamic

response of practical systems contains valuable information about the system including knowledge that could be used to develop an effective diagnostics framework. In an earlier work (Samadani, Kwuimy, & Nataraj, 2014, 2013) we presented an approach to extract information and features from the phase plane plot of the response in the periodic domain. The present paper extends that approach to systems with even more complex nonlinearities including quasi-periodicity using more advanced nonlinear dynamic analysis tools. The analysis in this paper is based on the recurrence properties of the system output in its reconstructed state space. In many cases, the phase space has dimensions higher than three which can only be visualized by projection into the two or three-dimensional sub-spaces. However, recurrence plots enable us to visualize and investigate certain aspects of the phase space trajectory in a two dimensional representation. The method of recurrence plots is a strong and effective tool for analysis of complex systems which has already been used for fault identification and diagnostics of nonlinear systems (Kwuimy, Samadani, Kappaganthu, & Nataraj, 2015). However, this is the first effort to use this method in a model-based approach to estimate the parameters of the system for fault diagnostics.

A detailed nonlinear mathematical model has been used to simulate the performance of the electro-hydraulic system. The analyses have been performed on the output flow of the servo valve. Three different electrical current signals including a periodic, a bi-periodic and a quasi-periodic signal have been input to the servo valve to investigate the performance of the algorithm in various nonlinear domains. RQA parameters have been obtained from the reconstructed phase space and used as the response features to identify dynamical changes in the system. Finally, an artificial neural network has been trained for mapping of the feature space to the parameter space.

The remaining parts of this paper are organized as follows. In section 2, a detailed mathematical model of the electro-hydraulic valve has been derived. In section 3, the definition of recurrence plots and RQA parameters have been provided. Section 4 describes the diagnostics algorithm along with the analyses and subsequent discussions. The conclusion is made in section 5.

2. MODELING OF THE ELECTRO-HYDRAULIC SERVO SYSTEM

A detailed dynamical model of a two-stage servo valve with a mechanical feedback has been used in the analyses. This system is shown in Fig. 1. Only the final equations are presented here. The detailed explanation of formulae can be found in (Samadani, Behbahani, & Nataraj, 2013; Rabie, 2009; Gordić, Babić, & Jovičić, 2004). The definition of system states and parameters along with the nominal values of the parameters have been presented in the nomenclature.

Neglecting the effect of the magnetic hysteresis, the net torque on the armature is given by the following expression.

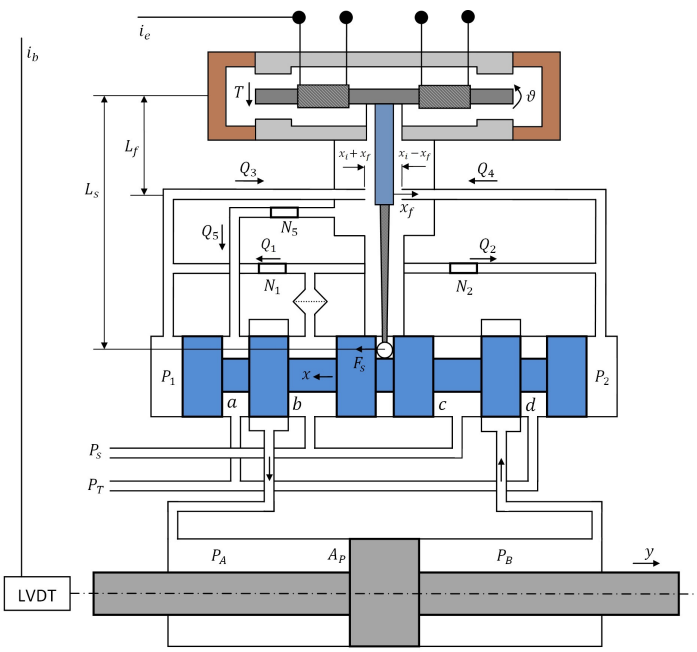

Figure 1. Functional schematic of the electro-hydraulic servo system [18]

$$T = K_i i_e \tag{1}$$

where the coefficient K_i can be calculated by:

$$K_i = \frac{N\lambda_p \mu_o A L}{2x_o^2} \tag{2}$$

The motion of the armature and the elements attached to it is described by the following equations:

$$T = J\frac{d^2\theta}{dt^2} + f_\theta \frac{d\theta}{dt} + K_T\theta + T_L + T_P + T_F \tag{3}$$

$$T_P = \frac{\pi}{4} d_f^2 (P_2 - P_1) L_f \tag{4}$$

The feedback torque depends on the displacement of the spool and the angle of the flapper and can be given by:

$$T_F = F_S L_S = K_S(L_S\theta + x)L_S \tag{5}$$

The rotational displacement of the flapper is limited mechanically by the jet nozzles. When the flapper reaches any of the side jet nozzles, a counter torque T_L is applied on it which can be calculated by the following equation:

$$T_L = \begin{cases} 0, & |x_f| < x_i \\ R_s \frac{d\theta}{dt} - (|x_f| - x_i) K_{Lf} L_f \text{sign}(x_f), & |x_f| > x_i \end{cases} \quad (6)$$

The flow rates through the flapper valve restrictions are given by the following equations:

$$Q_1 = C_D A_o \sqrt{\frac{2}{\rho}(P_s - P_1)} = C_{12}\sqrt{(P_s - P_1)} \quad (7)$$

$$Q_2 = C_D A_o \sqrt{\frac{2}{\rho}(P_s - P_2)} = C_{12}\sqrt{(P_s - P_2)} \quad (8)$$

$$\begin{aligned} Q_3 &= C_d \pi d_f (x_i + x_f)\sqrt{\tfrac{2}{\rho}(P_1 - P_3)} \\ &= C_{34}(x_i + x_f)\sqrt{(P_1 - P_3)} \end{aligned} \quad (9)$$

$$\begin{aligned} Q_4 &= C_d \pi d_f (x_i - x_f)\sqrt{\tfrac{2}{\rho}(P_2 - P_3)} \\ &= C_{34}(x_i - x_f)\sqrt{(P_2 - P_3)} \end{aligned} \quad (10)$$

$$x_f = L_f \theta \quad (11)$$

$$Q_5 = C_d A_s \sqrt{\frac{2}{\rho}(P_3 - P_T)} = C_5\sqrt{(P_3 - P_T)} \quad (12)$$

By using the continuity equation for the chambers of the flapper valve, the following expressions can be deduced:

$$Q_1 - Q_3 + A_s \frac{dx}{dt} = \frac{V_o - A_s x}{B}\frac{dP_1}{dt} \quad (13)$$

$$Q_2 - Q_4 - A_s \frac{dx}{dt} = \frac{V_o + A_s x}{B}\frac{dP_2}{dt} \quad (14)$$

$$Q_3 + Q_4 - Q_5 = \frac{V_3}{B}\frac{dP_3}{dt} \quad (15)$$

The motion of the spool is governed by the following equations.

$$A_s(P_2 - P_1) = m_s \frac{d^2x}{dt^2} + f_s \frac{dx}{dt} + F_j + F_s \quad (16)$$

$$F_j = \begin{cases} \left(\frac{\rho Q_b^2}{C_c A_b} + \frac{\rho Q_d^2}{C_c A_d}\right)\text{sign}(x) & \text{for } x > 0 \\ \left(\frac{\rho Q_a^2}{C_c A_a} + \frac{\rho Q_c^2}{C_c A_c}\right)\text{sign}(x) & \text{for } x < 0 \end{cases} \quad (17)$$

Ignoring the effect of transmission lines between the valve and the symmetrical hydraulic cylinder, the flow rates through the valve restriction areas are given by:

$$Q_a = C_d A_a(x)\sqrt{\frac{2}{\rho}(P_A - P_T)} \quad (18)$$

$$Q_b = C_d A_b(x)\sqrt{\frac{2}{\rho}(P_s - P_A)} \quad (19)$$

$$Q_c = C_d A_c(x)\sqrt{\frac{2}{\rho}(P_s - P_B)} \quad (20)$$

$$Q_d = C_d A_d(x)\sqrt{\frac{2}{\rho}(P_B - P_T)} \quad (21)$$

The area of the valve restrictions are given by:

$$\begin{cases} A_a = A_c = \omega c \\ A_b = A_d = \omega\sqrt{(x^2 + c^2)} \end{cases} \text{for } x \geq 0 \quad (22)$$

$$\begin{cases} A_a = A_c = \omega\sqrt{(x^2 + c^2)} \\ A_b = A_d = \omega c \end{cases} \text{for } x \leq 0 \quad (23)$$

Considering the internal leakage and neglecting the external leakage, the following equations can be obtained by applying the continuity equation to the cylinder chambers.

$$Q_b - Q_a - A_P\frac{dy}{dt} - \frac{(P_A - P_B)}{R_i} = \frac{(V_c + A_p y)}{B}\frac{dP_A}{dt} \quad (24)$$

$$Q_c - Q_a d + A_P\frac{dy}{dt} - \frac{(P_A - P_B)}{R_i} = \frac{(V_c - A_p y)}{B}\frac{dP_B}{dt} \quad (25)$$

Finally, the equation of motion for the cylinder piston is given by:

$$A_P(P_A - P_B) = m_p\frac{d^2y}{dt^2} + f_P\frac{dy}{dt} + K_b y \quad (26)$$

2.1. Servo Valve Faults

Various faults leading to parameter changes can appear in a servo valve. Three of the common defects in servo valves are:

- Change of magneto-motive force of the permanent magnet λ_p over time, which leads to the change of K_i
- Change of spool friction coefficient f_s, due to clearance variations or contamination

- Decrease in the diameter of nozzles d_f due to contamination or residuals

Sensitivity analyses show that the change of d_f does not significantly affect the dynamics of the system and hence, cannot be captured by dynamical analysis, unless the contamination blocks the nozzles completely. In this research, we assume the first two faults and use the response of the system in order to identify changes in those parameters. We suppose that one can measure the position of cylinder and the output flow of the valve.

3. RECURRENCE PLOTS AND RECURRENCE QUANTIFICATION ANALYSIS

The recurrence plots analysis for time series is based on the analysis of a matrix $\mathbf{R}$ whose elements are defined as:

$$\mathbf{R}_{ij} = \begin{cases} 1, & \mathbf{\Phi}_i \approx \mathbf{\Phi}_j, \\ 0, & \mathbf{\Phi}_i \neq \mathbf{\Phi}_j, \end{cases}, \quad i,j = 1...N, \tag{27}$$

where $\mathbf{\Phi}_i = (\phi_{1i}, \phi_{2i}, ..., \phi_{mi})$ is a state vector the dimension of m, N is the length of the time series, i and j are related respectively to the row and column of the matrix, and $\mathbf{\Phi}_i \approx \mathbf{\Phi}_j$ means equality up to an error ϵ.

If only a time series is available, the state vector $\mathbf{\Phi}$ can be reconstructed by using delay embedding theorem (Takens, 1981; Abarbanel, 1996; Fontaine, Dia, & Renner, 2011; Kwuimy, Samadani, & Nataraj, 2014). In this paper, the state vector has been reconstructed from the output flow of the valve. This is done in two steps: The first step consists of estimating the prescribed time lag T and the second step would be the evaluation of the embedded dimension m. In practice, if $u(i)$ is the available time series, the value of T corresponds to the first minimum of the average mutual information between the values of $u(i)$ and $u(i+T)$, and the embedding dimension can be deduced from the method of false nearness neighbor (Takens, 1981; Abarbanel, 1996; Kantz & Schreiber, 2004; Kwuimy et al., 2014). Once the values of T and m are obtained, the state vector $\mathbf{\Phi}$ can be reconstructed by:

$$\mathbf{\Phi} = (u(i), u(i+T), \ldots, u(i+T(m-1)) \tag{28}$$

The elements of the matrix $\mathbf{R}$ are thus obtained by comparing the state of the system at time i and j with a threshold precision ϵ. Thus, formally, one has:

$$\mathbf{R}_{ij} = \theta(\epsilon - ||\mathbf{\Phi}_i - \mathbf{\Phi}_j||), \tag{29}$$

with $||.||$ been the Euclidian norm (L_2-norm) and $\theta(y)$ is the heaviside function defined as:

$$\theta(y) = 1 \text{ for } y > 0 \text{ and } \theta(y) = 0 \text{ for } y < 0$$

Once we have the $\mathbf{R}$ matrix, the RP graph is obtained by plotting the R_{ij} points in the i and j plane with different colors. By definition, RP graphs are always symmetric ($R_{ij} = R_{ji}$) and always have a central diagonal.

In order to go beyond the qualitative impression given by RPs, complexity measures have been developed that quantify the structures of RPs and are called recurrence quantification analysis (RQA) (Zbilut, Thomasson, & Webber, 2002). In this paper, we use the following RQA parameters to quantify the RP of the system under various fault conditions.

- Recurrence rate (RR)

  The recurrence rate is the simplest RQA parameter which measures the density of recurrence points in a recurrence plot.

  $$RR = \frac{1}{N^2} \sum_{i,j=1}^{N} \mathbf{R}_{i,j}(\epsilon) \tag{30}$$

- Determinism (DET)

  The determinism is the percentage of recurrence points which form diagonal lines in the recurrence plot of minimal length $\ell_{\min}$.

  $$DET = \frac{\sum_{\ell=\ell_{min}}^{N} \ell P(\ell)}{\sum_{\ell=1}^{N} \ell P(\ell)} \tag{31}$$

  where $P(\ell)$ is the frequency distribution of the lengths ℓ of the diagonal lines.

- Laminarity (LAM)

  In the same way, the amount of recurrence points forming vertical lines can be quantified by laminarity.

  $$LAM = \frac{\sum_{v=v_{min}}^{N} v P(v)}{\sum_{v=1}^{N} v P(v)} \tag{32}$$

  where $P(v)$ is the frequency distribution of the lengths v of the vertical lines, which have at least a length of $v_{\min}$.

- Average length of the diagonal lines (L)

  L is related with the predictability time of the dynamical system.

  $$L = \frac{\sum_{\ell=\ell_{min}}^{N} \ell P(\ell)}{\sum_{\ell=\ell_{min}}^{N} P(\ell)} \tag{33}$$

- Trapping Time (TT)

  The trapping time measures the average length of the vertical lines.

$$TT = \frac{\sum_{v=v_{min}}^{N} vP(v)}{\sum_{v=v_{min}}^{N} P(v)} \tag{34}$$

- Entropy ($ENTR$)

  The probability that a diagonal line has exactly length ℓ can be estimated with $p(\ell) = \frac{P(\ell)}{\sum_{\ell=\ell_{\min}}^{N} P(\ell)}$. $ENTR$ is the Shannon entropy of this probability which reflects the complexity of the RP in respect of the diagonal lines.

$$ENTR = -\sum_{\ell=\ell_{min}}^{N} p(\ell)\ln p(\ell) \tag{35}$$

4. FAULT DIAGNOSTICS AND SEVERITY ANALYSIS

A standard procedure to identify faults and dynamical changes in systems is to input a pre-specified signal to the system, obtain the response and compare the signatures of the response with the ones of the system response in healthy conditions. Here we have input an electrical current signal to the servo valve, and measured the output flow of the valve. The state space of the system has then been reconstructed from the output flow signal and the effect of the parameter changes on the response has been evaluated using the defined recurrence quantification parameters.

In order to investigate the effectiveness of the approach in various domains of the nonlinear response, three different signals have been input to the servo valve including:

- Periodic input signal

$$i = 0.01\sin 50t$$

- Bi-periodic input signal

$$i = 0.01\sin 50t + 0.005\sin 75t$$

- Quasi-periodic input signal

$$i = 0.01\sin 50t + 0.005\sin 50\pi t$$

To better understand the effect of dynamical changes in recurrence point of view, the performance of the system is first analyzed and presented under three sample fault cases including:

- Healthy system
- Fault 1: K_i decreased by %50
- Fault 2: f_s increased by %500

Figure 2 shows the output flow of the valve versus time, corresponding to the three input cases, for the three sample fault scenarios.

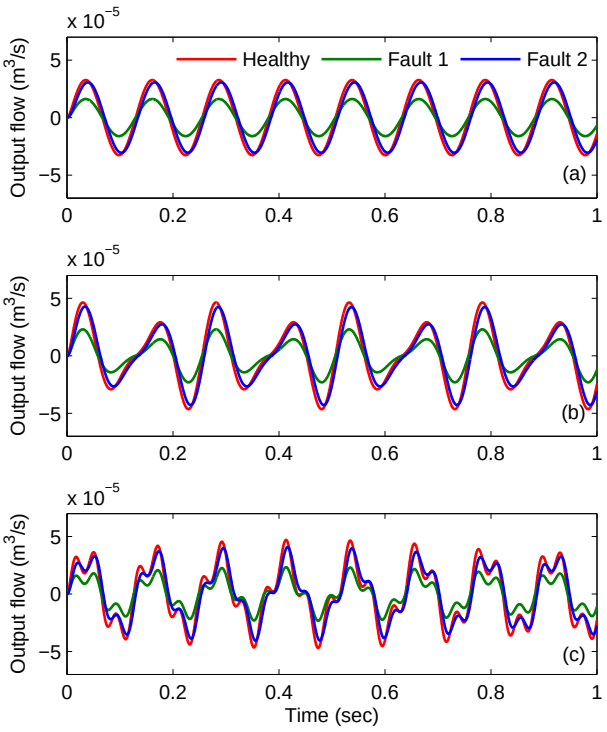

Figure 2. Time response of the system for (a): periodic, (b): bi-periodic and (c):quai-periodic inputs to the servo valve for three fault cases

In order to obtain the recurrence matrix and plots, we need to reconstruct the state space from the output flow time series. As discussed earlier, the appropriate time lag for the reconstruction of the state space corresponds to the first minimum in the average mutual information of the signal. Using this method, the time lag was determined to be T=50. By application of the method of false nearest neighbors, we found that the minimum embedding dimension for the system is d=2.

Figure 3 shows the recurrence plots of the reconstructed state space, for the three inputs and the three sample fault scenarios.

As can be seen, the plots consist of complicated patterns which are hard to interpret. In addition, there is little difference between them for the three fault cases, which is not easily detectable. Hence, we need quantitative measures to extract information from these plots.

Table 1 shows the computed RQA parameters for all nine cases. In this table p, bp, and qp correspond to the response of the system to the periodic, bi-periodic and quasi-periodic input signals, respectively. As can be seen, even though the difference of the recurrence plots for the three fault cases is hardly detectable by eye, RQA parameters can easily distinguish the differences and detect the alternations in the signal.

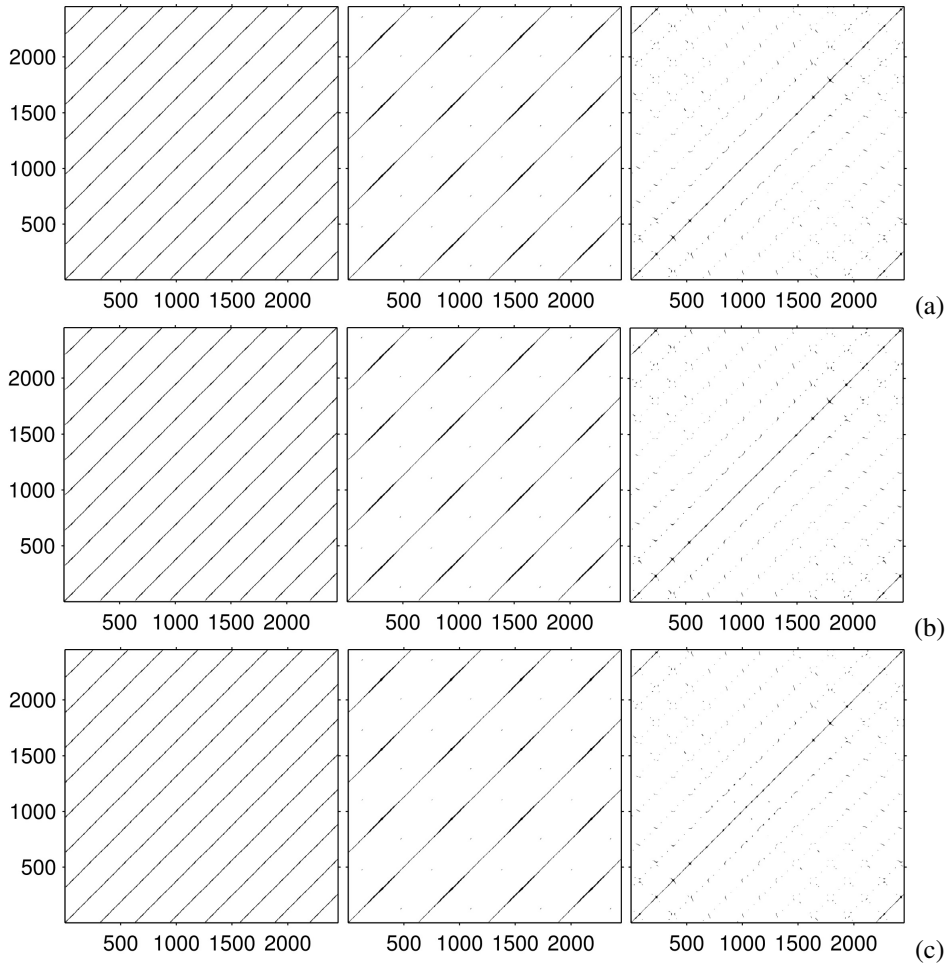

Figure 3. From left to right: Recurrence plots for periodic, bi-periodic and quasi-periodic inputs to the valve (a): Healthy system (b): Fault 1 (c): Fault 2

Table 1. RQA parameters for three defect cases

	Defect-free			Defect 1			Defect 2		
RQA Parameter	p	bp	qp	p	bp	qp	p	bp	qp
RR	0.0269	0.0160	0.0071	0.0269	0.0159	0.0070	0.0266	0.0160	0.0081
DET	0.9997	0.9994	0.9589	0.9997	0.9996	0.9589	0.9994	0.9996	0.9772
LAM	0.9999	0.9993	0.9548	0.9999	0.9993	0.9530	0.9997	0.9992	0.9790
L	107.1795	102.6667	5.6023	87.2343	95.2610	5.5580	103.0904	104.3878	6.7376
TT	7.4741	7.7383	4.4261	7.4741	7.7383	4.4261	7.4678	7.7575	4.9349
$ENTR$	3.7933	3.9199	1.9403	3.7933	3.9199	1.9403	3.8093	3.9572	2.2226

4.1. Mapping of Features to Parameters

So far we have illustrated how the response of the system is affected with the change of parameters and how it can be detected by using the RQA parameters. We were able to measure and represent these influences by quantitative criteria. In contrast to this, the diagnostics problem is the inverse problem, where we would like to predict the system parameters given its nonlinear response. In order to do that, machine learning techniques can be used which have been proved to be effective for diagnostics of machinery (Kankar, Sharma, & Harsha, 2011) and biomedical diagnostics (Jalali et al., 2014). In this paper, an artificial neural network (ANN) has been used. For this purpose, a two-layer feed-forward network with ten sigmoid hidden neurons and linear output neurons was developed. The inputs used for the training of the neural network were vectors of RQA parameters and the outputs were vectors of K_i and f_s. The data was obtained by random selection of the values of K_i and f_s in the intervals [0.1,0.6] and [1,100], respectively, simulation of the system and computation of the response features, i.e. RQA parameters, each time. A total number of 100 samples was used for training, validation and test of the network.

Figures 4, 5, and 6 show the regression plots of the network outputs with respect to targets for training, validation and test sets along the Regression (R) values for each case. For a perfect fit, the (R) value should be close to 1 and the data in the regression plot should fall along a 45 degree line, where the network outputs are equal to the targets. As can be seen, in this case, all the points have fallen along the 45 degree line and the R values are equal to 1, which are representatives of an accurate mapping of the features space to the parameters space.

Table 2 shows some samples of the performance of the parameter estimation systems developed with periodic, bi-periodic and quasi-periodic inputs. K_i^* and f_s^* represent the estimated values of K_i and f_s. This table shows that the proposed method has a very good ability to predict the original parameters of the system using the defined features, especially with the periodic input signal.

Table 2. Some examples of the performance of the parameter estimation system

		Periodic		Bi-periodic		Quasi-periodic	
K_i	f_s	K_i^*	f_s^*	K_i^*	f_s^*	K_i^*	f_s^*
0.1	5	0.098	5.879	0.096	6.087	0.123	6.088
0.3	50	0.289	50.623	0.275	51.025	0.356	51.610
0.6	100	0.591	101.511	0.592	98.410	0.633	102.214
0.2	25	0.207	24.234	0.206	25.324	0.227	26.665
0.4	2	0.390	2.012	0.384	2.622	0.383	3.001
0.5	10	0.512	9.824	0.488	9.357	0.520	9.512

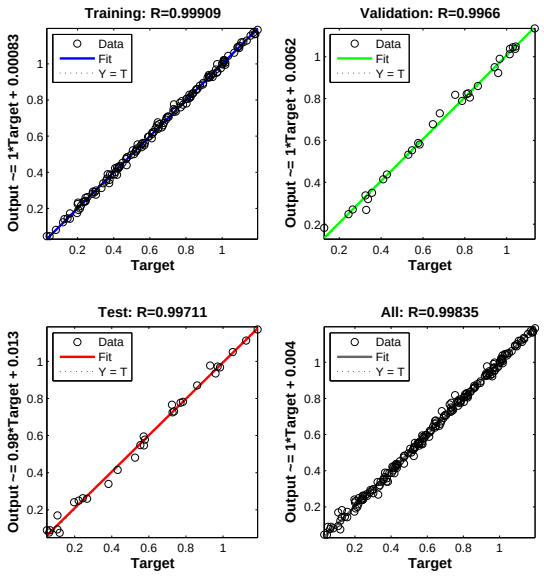

Figure 4. Outputs of the artificial neural network with respect to target values for the periodic input signal

5. CONCLUSION

We used recurrence plots and recurrence quantification analysis for model-based fault detection and diagnostics of an electro-hydraulic system. It was shown that the nonlinear response of the system contains valuable information about the system that can be used for this purpose. The analyses were performed with the assumption that only the output response of the system (here output flow of the valve) is available; and the other states were reconstructed using the method of time delays. The recurrence plots were produced and the corresponding recurrence analyses were performed on the reconstructed state space of the system. It was shown that even though the recurrence plots for the system with different faults can be similar, the dynamical changes can be detected by RQA parameters. An artificial neural network was trained using the RQA parameters to estimate the faulty parameters of the system. It was shown that RQA parameters can be used as effective features for characterizing the nonlinear response of the system even in the multi-periodic or quasi-periodic domain with complex nonlinearities.

In this study, the proposed method was only applied to numerical data obtained from the mathematical model of the system. Although the results were promising, there is no guarantee that we can obtain the same prediction accuracy for real experimental data. Hence, it is of importance to confirm the effectiveness of the approach with experimental analysis. In addition, only two parametric defects (defects due to change of parameter values) were considered in this paper, whereas in real world applications we might have multiple paramet-

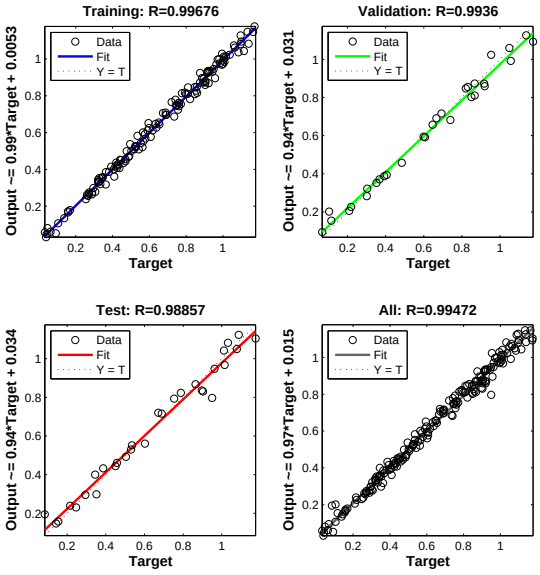

Figure 5. Outputs of the artificial neural network with respect to target values for the bi-periodic input signal

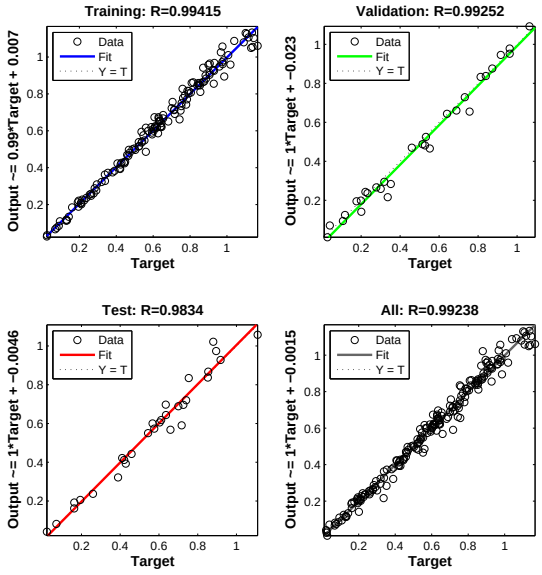

Figure 6. Outputs of the artificial neural network with respect to target values for the quasi-periodic input signal

ric defects in the system or even defects of the type that can change the structure of the mathematical model of the system. The present method can be extended with using more dynamical and statistical features in order to be able to characterize the system response and diagnose the faults in such conditions, which is currently the focus of our research.

ACKNOWLEDGMENT

This work is supported by the US Office of Naval Research under the grant ONR N00014-13-1-0485. We deeply appreciate this support. Thanks are due to Mr Anthony Seman III of ONR.

NOMENCLATURE

a	Width of spool edges	m	4e-03
A	Area of air gap	m^2	
A_5	Drain orifice area	m^2	
A_L	Area of the flow between spool and sleeve edges	m^2	
A_o	Orifice area	m^2	
$A_{a'}$, $A_{b'}$, $A_{c'}$, and $A_{d'}$	Spool valve restrictions areas	m^2	
A_P	Piston area	m^2	7e-04
A_s	Spool cross-sectional area	m^2	
b	Width of sleeve slots	m	4e-03
B	Bulk modulus of oil	Pa	1.5e09
c	Spool radial clearance	m	2e-06
C_c	Contraction coefficient		
C_d and C_D	Discharge coefficients		0.661
d_f	Flapper nozzle diameter	m	5e-04
d_5	Diameter of return orifice	m	6e-04
d_s	Spool diameter	m	4.6e-03
f_θ	Armature damping coefficient	Nms/rad	0.002
F_j	Hydraulic momentum force	N	
f_p	Piston friction coefficient	Ns/m	1000
f_s	Spool friction coefficient	Ns/m	3.05
F_s	Force acting at the extremity of the feedback spring	N	
H	Magneto-motive force per unit length	A/m	
i_b	Feedback current	A	
i_c	Control current	A	
i_e	Torque motor input current	A	
J	Moment of inertia of rotating part	Nms^2	5e-07
K_b	Load coefficient	N/m	0
K_{FB}	Feedback gain	A/m	1
K_{Lf}	Equivalent flapper seat stiffness	N/m	1e6
K_i	Current-torque gain	Nm/A	0.559
K_s	Stiffness of the feedback spring	N/m	900
K_T	Stiffness of flexure tube	Nm/rad	10.68
K	Rotational angle-torque gain	Nm/rad	9.45e-4
L	Armature length	m	0.029
L_f	Flapper length	m	0.009
L_s	Length of the feedback spring and flapper	m	0.03

L_{sp}	Length of spool land	m	1.5e-02
m_p	Piston mass	kg	5
m_s	Spool mass	kg	0.2
P_1	Pressure in the left side of the flapper valve	Pa	
P_2	Pressure in the right side of the flapper valve	Pa	
P_3	Pressure in the flapper valve return chamber	Pa	
P_A and P_B	Hydraulic cylinder pressures	Pa	
P_s	Supply pressure	Pa	1.2e7
P_T	Return line pressure	Pa	0
Q	Flow rate	m^3/s	
Q_1	Flow rate in the left orifice	m^3/s	
Q_2	Flow rate in the right orifice	m^3/s	
Q_3	Left flapper nozzle flow rate	m^3/s	
Q_4	Right flapper nozzle flow rate	m^3/s	
Q_5	Flapper valve drain flow rate	m^3/s	
Q_a, Q_b, Q_c, and Q_d	Flow rates through the spool valve restrictions	m^3/s	
R_i	Resistance to internal leakage	Ns/m^5	1e20
R_s	Flapper seat damping coefficient	$\mathrm{Nms}/\mathrm{rad}$	5000
T	Torque of electromagnetic torque motor	Nm	
T_F	Feedback torque	Nm	
T_L	Torque due to flapper displacement limiter	Nm	
T_P	Torque due to the pressure forces	Nm	
V_3	Volume of the flapper valve return chamber	m^3	5e-06
V_c	Half of the volume of oil filling the cylinder	m^3	1e-04
V_o	Initial volume of oil in the spool side chamber	m^3	2e-06
x	Spool displacement	m	
x_a	Displacement of the armature end	m	
x_f	Flapper displacement on the level of the jet nozzles	m	
x_i	Flapper displacement limit	m	3e-05
x_o	Length of the air gap in the neutral position of armature	m	3e-04
λ	Magneto-motive force	A	
λ_p	Magneto-motive force of the permanent magnet	A	66.75
μ	Permeability	Vs/Am	
μ_o	Permeability of the air	Vs/Am	4e-07
μ_r	Relative permeability		
ρ	Oil density	kg/m^3	867
ω	Width of ports on the valve sleeve	m	0.014
θ	Armature rotation angle	rad	

REFERENCES

Abarbanel, H. D. I. (1996). *Analysis of observed chaotic data*. Springer, New York.

Baskiotis, C., Raymond, J., & Rault, A. (1979). Parameter identification and discriminant analysis for jet engine machanical state diagnosis. In *18th IEEE Conference on Decision and Control including the Symposium on Adaptive Processes* (Vol. 18, pp. 648–650).

Chow, E., & Willsky, A. (1984). Analytical redundancy and the design of robust failure detection systems. *IEEE Transactions on Automatic Control*, *29*(7), 603–614.

Fontaine, S., Dia, S., & Renner, M. (2011). Nonlinear friction dynamics on fibrous materials, application to the characterization of surface quality. part i: global characterization of phase spaces. *Nonlinear Dynamics*, *66*(4), 625–646.

Frank, P., Ding, S. X., & Koppen-Seliger, B. (2000). Current developments in the theory of FDI. In *Proceedings of SAFEPROCESS* (Vol. 1, pp. 16–27).

Frank, P., & Ding, X. (1997). Survey of robust residual generation and evaluation methods in observer–based fault detection systems. *Journal of Process Control*, *7*(6), 403–424.

Gertler, J. (1997). Fault detection and isolation using parity relations. *Control Engineering Practice*, *5*(5), 653–661.

Gertler, J., & Singer, D. (1990). A new structural framework for parity equation–based failure detection and isolation. *Automatica*, *26*(2), 381–388.

Gordić, D., Babić, M., & Jovičić, N. (2004). Modelling of spool position feedback servovalves. *International Journal of Fluid Power*, *5*(1), 37–51.

Isermann, R. (1982). Parameter adaptive control algorithms–a tutorial. *Automatica*, *18*(5), 513–528.

Isermann, R. (1984). Process fault detection based on modeling and estimation methods–a survey. *Automatica*, *20*(4), 387–404.

Isermann, R. (1997). Supervision, fault-detection and fault-diagnosis methods–an introduction. *Control Engineering Practice*, *5*(5), 639–652.

Isermann, R. (2005a). *Fault-diagnosis systems: an introduction from fault detection to fault tolerance*. Springer.

Isermann, R. (2005b). Model-based fault-detection and diagnosis–status and applications. *Annual Reviews in Control*, *29*(1), 71–85.

Jalali, A., Buckley, E. M., Lynch, J. M., Schwab, P. J., Licht, D. J., & Nataraj, C. (2014, Jul). Prediction of periventricular leukomalacia occurrence in neonates after heart surgery. *IEEE Journal of Biomedical and Health Informatics*, *18*(4), 1453–1460.

Kankar, P., Sharma, S. C., & Harsha, S. (2011). Fault diagnosis of ball bearings using machine learning methods. *Expert Systems with Applications*, *38*(3), 1876–1886.

Kantz, H., & Schreiber, T. (2004). *Nonlinear time series analysis*. Cambridge University Press.

Kappaganthu, K., & Nataraj, C. (2011a). Mutual information based feature selection from data driven and model based techniques for fault detection in rolling element bearings. In *ASME 2011 International Design Engineering Technical Conferences and Computers and Information in Engineering Conference* (pp. 941–953).

Kappaganthu, K., & Nataraj, C. (2011b). Nonlinear modeling and analysis of a rolling element bearing with a clearance. *Communications in Nonlinear Science and Numerical Simulation*, *16*(10), 4134–4145.

Kwuimy, C. A. K., Samadani, M., Kappaganthu, K., & Nataraj, C. (2015). Sequential recurrence analysis of experimental time series of a rotor response with bearing outer race faults. In *Vibration engineering and technology of machinery* (pp. 683–696). Springer.

Kwuimy, C. A. K., Samadani, M., & Nataraj, C. (2014). Preliminary diagnostics of dynamic systems from time series. In *Proceedings of the ASME International Design Engineering Technical Conference.*

Liu, X.-Q., Zhang, H.-Y., Liu, J., & Yang, J. (2000). Fault detection and diagnosis of permanent-magnet DC motor based on parameter estimation and neural network. *IEEE Transactions on Industrial Electronics*, *47*(5), 1021–1030.

Mevel, B., & Guyader, J. (1993). Routes to chaos in ball bearings. *Journal of Sound and Vibration*, *162*(3), 471–487.

Patton, R. J., Frank, P. M., & Clarke, R. N. (1989). *Fault diagnosis in dynamic systems: theory and application*. Prentice–Hall, Inc.

Rabie, M. (2009). *Fluid power engineering*. McGraw Hill Professional.

Samadani, M., Behbahani, S., & Nataraj, C. (2013). A reliability-based manufacturing process planning method for the components of a complex mechatronic system. *Applied Mathematical Modelling*, *37*(24), 9829–9845.

Samadani, M., Kwuimy, C. A. K., & Nataraj, C. (2013). Diagnostics of a nonlinear pendulum using computational intelligence. In *ASME 2013 Dynamic Systems and Control Conference.*

Samadani, M., Kwuimy, C. A. K., & Nataraj, C. (2014). Model-based fault diagnostics of nonlinear systems using the features of the phase space response. *Communications in Nonlinear Science and Numerical Simulation*.

Sankaravelu, A., Noah, S. T., & Burger, C. P. (1994). Bifurcation and chaos in ball bearings. *ASME Applied Mechanics Division–Publications–AMD*, *192*, 313–313.

Takens, F. (1981). Detecting strange attractors in turbulence. In *Dynamical Systems and Turbulence* (pp. 366–381). Springer.

Zbilut, J. P., Thomasson, N., & Webber, C. L. (2002). Recurrence quantification analysis as a tool for nonlinear exploration of nonstationary cardiac signals. *Medical Engineering & Physics*, *24*(1), 53–60.

BIOGRAPHIES

Mohsen Samadani Mohsen received his B.Sc and M.Sc in Mechanical Engineering from Isfahan University of Technology, Isfahan, Iran. He is currently a Ph.D. candidate at the Department of Mechanical Engineering at Villanova University. Mohsen has been involved in various research topics including manufacturing technologies, control, vibrations, system dynamics, hydraulic systems and reliability analysis. His current research interests include data analysis, machine learning, nonlinear dynamics and vibrations with applications to machinery diagnostics and health management. He is a member of Sigma Xi and ASME and a recipient of Sigma Xi best poster award and PHM doctoral consortium travel award.

Cedrick Kwuimy Prior to joining the Department of Mechanical Engineering at Villanova University in Jan. 2011, Dr. Kwuimy worked in South Africa as a postdoctoral research associate at the African Institute for Mathematical Sciences (2009-2010) and as a Research and Teaching Assistant (2007-2009) at the Faculty of Science at the University of Yaounde, Cameroon. He has been involved in a wide range of research topics including vibration control, nonlinear dynamics of self-sustained electromechanical devices, synchronization, nonlinear analysis of butterfly valves, and chaos control and prediction in active magnetic bearings. He has over 30 peer-reviewed papers in international journals and conference proceedings and serves as a reviewer in high standard journals including Nonlinear Dynamics, Journal of Vibration and Control and Journal of Sound and Vibration. Dr. Kwuimy has supervised three graduate research theses at the African Institute for Mathematical Sciences and is the recipient of Victor Rothschild Fellowships at African Institute for Mathematical Sciences and Research.

C. Nataraj Dr. C. Nataraj holds the Mr. and Mrs. Robert F. Mortiz, Sr. Endowed Chair Professorship in Engineered Systems at Villanova University. He has a B.S. in Mechanical Engineering from Indian Institute of Technology, and M.S. and Ph.D. in Engineering Science from Arizona State University. After getting his Ph.D. in 1987, he worked for a year as a research engineer and a partner with Trumpler Associates, Inc. He is currently the Chairman of the Mechanical Engineering Department at Villanova University. Dr. Nataraj was also the founding director of the Center for Nonlinear Dynamics and Control in the College Of Engineering. He has worked on various research problems in nonlinear dynamic systems with applications to mobile robotics, unmanned vehicles, rotor dynamics, vibration, control, and electromagnetic bearings. His research has been funded by Office of Naval Research, National Science Foundation, National Institute of Health and many companies.